Introducing the Enhanced Cervical Cancer Detection Model PapEMS-Net, Integrating EfficientNet, Multi-Verse Optimizer, and Softmax Entropy Classifier

M. Sandhya Vani
Department of Computer Science and Engineering, Koneru Lakshmaiah Education Foundation, Hyderabad-500075, Telangana, India
msandhyavani4@gmail.com

N. Rama Rao
Department of Computer Science and Engineering, Koneru Lakshmaiah Education Foundation, Hyderabad-500075, Telangana, India
ramarao.n@klh.edu.in (corresponding author)

Received: 24 June 2025 | Revised: 19 August 2025 | Accepted: 30 August 2025

 DOI: https://doi.org/10.48084/etasr.12917

ABSTRACT

Cervical cancer remains a leading cause of mortality in low-resource regions where early diagnosis is often delayed due to limited access to expert cytologists and manual screening methods. To address the need for a robust, automated diagnostic system, this study proposes PAP smear EfficientNet-MVO-Softmax classifier Network (PapEMS-Net), a deep learning-based architecture designed for accurate classification of cervical cell types in PAP smear images. This study introduces PapEMS-Net, a deep learning framework designed to classify cervical cells in PAP smear images. By combining EfficientNet, Multi-Verse Optimizer (MVO), and a Softmax Entropy Classifier, the model provides accurate and efficient classification. The proposed PapEMS-Net model, evaluated on the Single-cell PAP Smear Image Dataset for Medical Diagnosis (SIPaKMeD), achieved an accuracy of 99.43%, precision of 99.29%, recall of 99.37%, and F1-score of 99.31%, outperforming existing models. The visual analysis through confusion matrix, ROC curves, and predicted class distributions further validated the model's discriminative capability across all five cytological classes.

Keywords-cervical cancer; PAP smear; accuracy; optimization; deep learning; detection

I. INTRODUCTION

Cervical cancer is one of the most prevalent and life-threatening diseases affecting women globally, especially in developing regions, where regular screening and access to expert cytologists remain limited [1-4]. Despite the availability of effective prevention and treatment methods, delayed diagnosis due to manual error-prone screening continues to contribute significantly to the mortality rates [5]. The PAP smear test is a widely used and effective method for early detection of cervical abnormalities; however, its manual analysis is labor-intensive, subjective, and prone to inter-observer variability [6-9]. This creates a need for reliable, automated diagnostic solutions that can assist pathologists in identifying precancerous and cancerous cells with high precision and consistency [10-13].

The integration of artificial intelligence, particularly deep learning, into medical image analysis has shown significant promise in transforming diagnostic accuracy and speed [14-17]. Deep Convolutional Neural Networks (CNNs) have the ability to learn and extract complex spatial patterns from histological and cytological images, making them suitable for automated PAP smear analysis [18-20]. However, challenges, such as the inter-class similarity of cell types, presence of overlapping structures, and the need for interpretability in clinical environments require robust model design and optimization [21]. Furthermore, to ensure its practical usability, the system must maintain high accuracy across multiple cytological classes while remaining computationally efficient for real-world deployment [22].

To address these challenges, this study proposes a novel deep learning architecture named PapEMS-Net, which combines the scalable feature extraction power of EfficientNet, the optimization strength of the MVO for feature selection, and the probabilistic decision-making of a Softmax Entropy Classifier.

II. RELATED WORKS

Authors in [23] proposed a hybrid deep learning model by integrating the ResNet-50 and VGG-19 architectures for cervical cancer classification. However, the dual-model integration increased computational complexity and model size, which may hinder real-time diagnostic deployment in low-resource settings.

Authors in [24] implemented an EfficientNet model augmented with an attention mechanism to prioritize salient regions within PAP smear images. Despite their high performance, the use of attention mechanisms introduces added layers of computation, which can increase training time and require more tuning for different datasets. Authors in [25] adopted a deeper ResNet-152 model for feature extraction in cervical image classification.

Also, authors in [26] proposed CCanNet, an ensemble framework. However, the fusion of CNN and ViT components led to a relatively complex model architecture that demands substantial computational resources and extended training times. Authors in [27] applied SqueezeNet, a lightweight convolutional architecture, to address cervical cell classification. Yet, this simplification came at the cost of lower classification accuracy compared to deeper models, limiting its effectiveness in detecting subtle abnormalities in complex cellular samples. Subsequently, authors in [28] introduced a Graph Convolution Network (GCN) approach, which achieved significantly better results with 99.11% accuracy. Authors in [29] also made significant contributions by employing DenseNet-121 integrated with a self-attention mechanism. Although this combination performed well, the memory overhead associated with DenseNet and attention layers makes the model less suitable for lightweight diagnostic platforms.

Finally, authors in [30] introduced the Mean and Standard Deviation-based Ensemble Network (MSENet) for cervical image analysis, achieving an accuracy of 97.21%. Although MSENet demonstrated robustness and high accuracy, it relied heavily on handcrafted ensemble techniques, which may not adapt well to newer datasets or unseen data patterns without significant retraining or manual adjustment.

III. PROPOSED SYSTEM

The proposed methodology framework shown in Figure 1 represents a pipeline process. In this work, the novel Pap-EMS-Net model is proposed, which integrates the EfficientNet deep learning architecture for robust and multi-scale feature extraction from high-resolution PAP smear images. To enhance the model's performance, the extracted features are further optimized using the MVO, a nature-inspired metaheuristic algorithm that effectively selects the most relevant and discriminative features. This feature selection process reduces redundancy and improves classification accuracy. Finally, a Softmax Entropy Classifier is employed to assign the optimized features to their respective classes, enabling accurate identification of cellular abnormalities in cervical smear images.

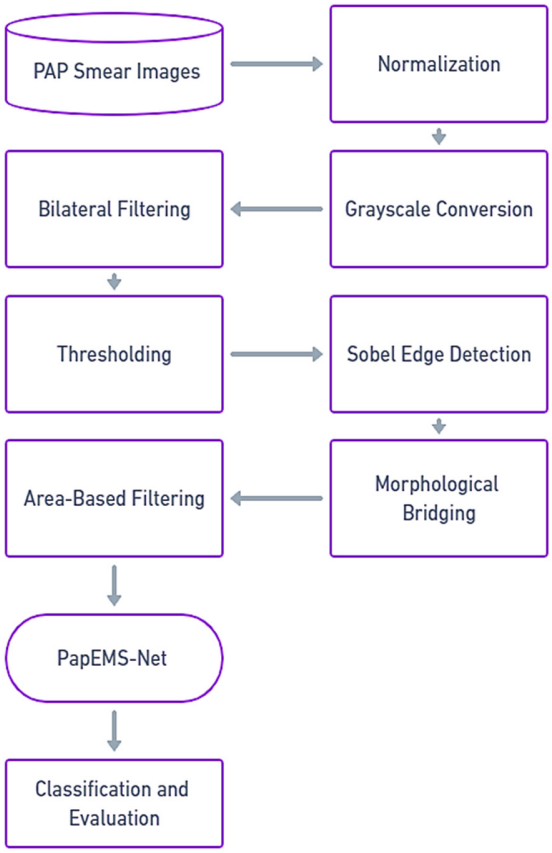

Fig. 1. Proposed methodology framework.

Let the dataset of high-resolution PAP smear images be denoted as:

$$I = \{I_1, I_2, \dots \dots \dots, I_N\} \quad (1)$$

where $I_i \in \mathbb{R}^{H\times W\times 3}$ H and W represent the height and width of the image, respectively. Each image is normalized to maintain consistency.

$$I_i' = \frac{I'-\mu}{\sigma} \quad (2)$$

where μ and σ are the mean and standard deviation of image intensities across the dataset.

Each RGB image is converted into grayscale using:

$$G(x,y) = 0.2989 \cdot R(x,y) + 0.5870 \cdot G(x,y) + 0.1140 \cdot B(x,y) \quad (3)$$

Let $G_i \in \mathbb{R}^{H\times W}$ denote the grayscale image for each I'_i.

- Bilateral Filtering: The bilateral filter smoothens the image while preserving the edges:

$$G^f(p) = \frac{1}{W_p} \sum_{q\in\Omega} G(q) \cdot exp\left(-\frac{\|p-q\|^2}{2\sigma_s^2} - \frac{|G(p)-G(q)|^2}{2\sigma_r^2}\right) \quad (4)$$

where p and q are pixel locations, σ_s is the spatial standard deviation, σ_r is the range standard deviation, and W_p is a normalization factor.

- Intensity-based Thresholding: Binary thresholding is used to isolate cytoplasmic and nuclear regions:

$$T(x,y) = \begin{cases} 1, & \text{if } G^f(p) \geq \tau \\ 0, & \text{otherwise} \end{cases} \quad (5)$$

where τ is an empirically selected threshold.

- Sobel Edge Detection: The gradient magnitude is computed using:

$$G_x = \frac{\partial G}{\partial x} \quad (6)$$

$$G_y = \frac{\partial G}{\partial y} \quad (7)$$

$$|G_{Sobel}(x,y)| = \sqrt{G_x^2 + G_y^2} \quad (8)$$

where kernels are used to compute G_x and G_y.

- Bridging connects broken boundaries using morphological closing:

$$B = (T \oplus S) \ominus S \quad (9)$$

where $\oplus$ and $\ominus$ denote dilation and erosion, S denotes a structuring segment.

- Area-based Filtering: All connected components $C_j \subseteq B$ are filtered by:

$$C_j = \begin{cases} 0, & if\ Area\ C_j < \theta \\ C_j, & otherwise \end{cases} \quad (10)$$

where θ is the minimum area threshold to remove artifacts.

- EfficientNet Feature Extraction: Given an image I, the CNN extracts multi-scale hierarchical features:

$$F = f_{EfficientNet}(I) \quad (11)$$

where $F \in \mathbb{R}^d$ is a feature vector, and d is the feature dimension.

Let $X_i = \{x_1, x_2, \ldots\ldots\ldots, x_d\}$ be a candidate feature vector, then $f(X_i)$ is the fitness score. MVO updates each universe (solution vector) using white hole and wormhole mechanisms:

$$x_j^{i,t+1} = \begin{cases} x_j^{k,t}, & \text{if } r_1 < NI(i) \\ x_j^{i,t} + TDR \cdot (ub_j - lb_j) \cdot r_2, & \text{if } r_3 < WEP \\ x_j^{i,t} - TDR \cdot (ub_j - lb_j) \cdot r_2, & \text{if otherwise} \end{cases} \quad (12)$$

where *NI(i)* is the normalized inflation rate, *WEP* is the wormhole existence probability, *TDR* is the travelling distance rate, ub_j and lb_j are the upper and lower bounds of dimension *j*, respectively, and $r_1, r_2, r_3 \sim \mathcal{U}(0,1)$.

- Softmax Entropy Classifier: Given selected features $F_s \in \mathbb{R}^k$ class scores are:

$$z_i = W_i \cdot F_s + b_i \quad (13)$$

The Softmax output for class *i* is:

$$P(y = i|F_s) = \frac{e^{z_i}}{\sum_{j=1}^{C} e^{z_j}} \quad (14)$$

The classification loss (cross-entropy) is:

$$\mathcal{L} = -\sum_{i=1}^{C} y_i \log\left(P(y = i \mid F_s)\right) \quad (15)$$

where *C* is the number of classes.

A. *Proposed Model*

The proposed PapEMS-Net model, as depicted in Figure 2, is an ensembled architecture tailored for accurate classification of cervical cells in PAP smear images. At its core, the model employs EfficientNet as the feature extraction backbone due to its compound scaling strategy, which uniformly scales depth, width, and resolution using a predefined coefficient. EfficientNet efficiently balances computational cost with accuracy, making it ideal for handling high-resolution cytological images. The backbone network receives pre-processed grayscale input images and passes them through a series of convolutional layers, batch normalization layers, and swish activation functions. Following the feature extraction, the high-dimensional feature vector output from EfficientNet is processed by an MVO module.

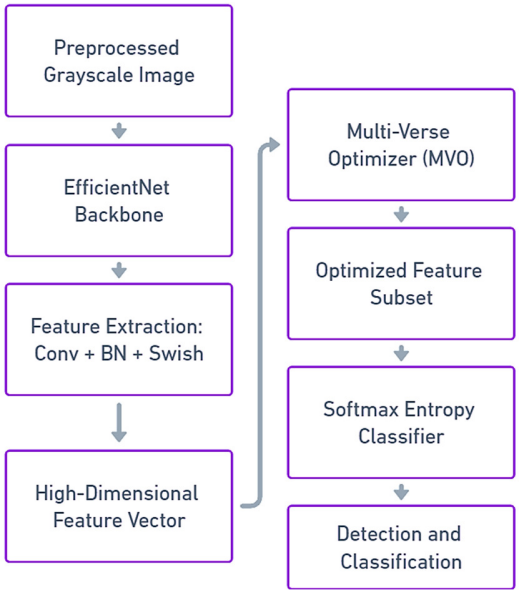

Fig. 2. PapEMS-Net model architecture.

In MVO, each solution represents a feature subset, and its fitness is evaluated based on classification accuracy. Through operations analogous to white holes, black holes, and wormholes, the algorithm performs exploration and exploitation, refining the selected features while preserving the integrity of important spatial structures. The key contribution of PapEMS-Net lies in its hybrid design that integrates EfficientNet for multi-scale feature extraction, the MVO for intelligent feature selection, and a Softmax Entropy Classifier for accurate multiclass categorization. This combination ensures high precision, robustness, and computational efficiency compared to existing methods.

B. Algorithm of the Proposed Model

The PapEMS-Net model algorithm integrates EfficientNet for deep hierarchical feature extraction and leverages the MVO to intelligently select the most informative features.

```
Algorithm: PapEMS-Net Model
Step 1:  Input Preprocessed Image
Step 2:  Feature Extraction using
         EfficientNet
Step 3:  Initialize MVO
Step 4:  Feature Selection using MVO
           % Perform white hole and
           wormhole updating
           (probabilistic update)
Step 5:  Classification using Softmax
         Entropy Classifier
           % Fully connected layer +
           softmax
Step 6:  Output Class Prediction
           [~, y_pred] = max(P_class);
           % Index of maximum probability
```

IV. RESULTS AND DISCUSSION

SIPaKMeD [31] presented in Table I serves as a valuable benchmark for the development and validation of automated cervical cell classification systems. It comprises a total of 4049 isolated cell images, manually cropped from 966 multi-cell PAP smear images. These images were acquired using a CCD camera (Infinity 1 by Lumenera) attached to an OLYMPUS BX53F optical microscope, ensuring high-resolution and uniform imaging standards across all samples [31].

TABLE I. SIPAKMED DATASET OVERVIEW

Parameter	Value
Cluster images	966
Isolated cells	4049
Device	CCD (infinity 1)
Microscope	Olympus BX53F
Image type	RGB (grayscale during preprocessing)
Usage	Classification of cervical epithelial cells

The individual class distribution of isolated cells is outlined in Table II, highlighting the representation of each type. This breakdown facilitates the balanced training of classification algorithms, particularly for multiclass models that require equitable sampling of different categories. Figure 3 illustrates the overall distribution of isolated cervical cells across the five categories in the SIPaKMeD dataset. Each segment in the donut chart represents the proportion of Superficial/Intermediate, Parabasal, Koilocytotic, Metaplastic, and Dyskeratotic cells out of the total 4049 samples. The chart confirms a relatively balanced representation, which is essential for unbiased training of classification models.

This 70:30 division, as shown in Table III, provides a balanced framework to train models like PapEMS-Net, ensuring sufficient samples per class during training while retaining a diverse and representative testing set for validation.

Figure 4 displays the dataset partitioning into training and testing sets using a 70:30 ratio. Figure 4(a) depicts the training set distribution, while Figure 4(b) represents the testing set. Figure 5 portrays a raw PAP smear image captured under a microscope, showing multiple overlapping and scattered epithelial cells. Figure 6 shows the grayscale version of the original image, where color components have been removed to focus solely on intensity information. Figure 7 displays the result of bilateral filtering applied to the grayscale image.

TABLE II. CLASS-WISE DISTRIBUTION OF ISOLATED CELLS

Cell category	Cluster images	Isolated cells
Superficial/intermediate	126	813
Parabasal	108	787
Koilocytotic	238	825
Metaplastic	271	793
Dyskeratotic	223	831
Total	966	4049

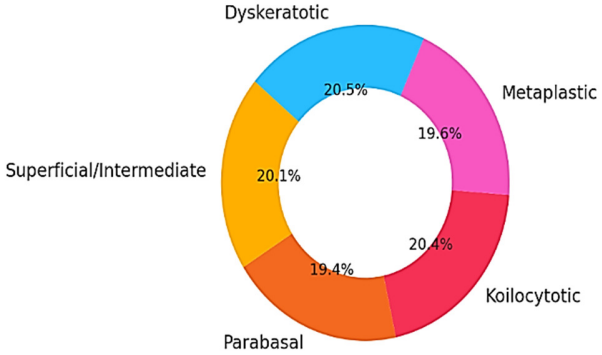

Fig. 3. Distribution of isolated cells.

TABLE III. SIPAKMED DATASET – 70:30 TRAIN-TEST SPLIT

Cell category	Total cells	Training set (70%)	Testing set (30%)
Superficial/intermediate	813	569	244
Parabasal	787	551	236
Koilocytotic	825	578	247
Metaplastic	793	555	238
Dyskeratotic	831	582	249
Total	4049	2835	1214

Figure 8 illustrates the output after applying intensity-based thresholding. In this stage, the cellular components are segmented from the background by assigning binary labels based on intensity levels. Figure 9 depicts the result of edge detection using the Sobel operator. Figure 10 shows the image after morphological bridging has been applied.

Figure 11 highlights the region of interest where abnormality has been detected. The region is marked based on morphological and textural features identified by the model.

(a)

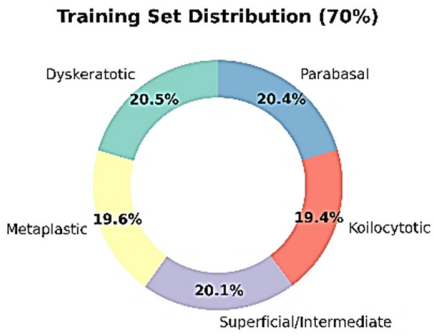

(b)

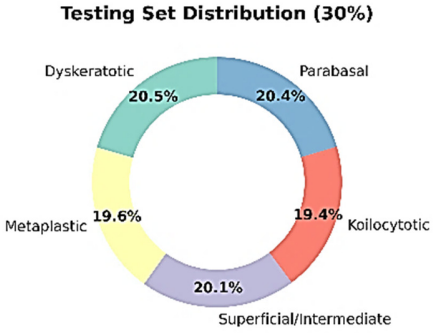

Fig. 4. Dataset distribution: (a) training, (b) testing.

Fig. 5. Original PAP smear image sample.

The confusion matrix in Figure 12 depicts the performance of the PapEMS-Net model on the SIPaKMeD test dataset. The matrix shows high accuracy across all five cell categories, with the majority of predictions concentrated on the diagonal, indicating correct classifications.

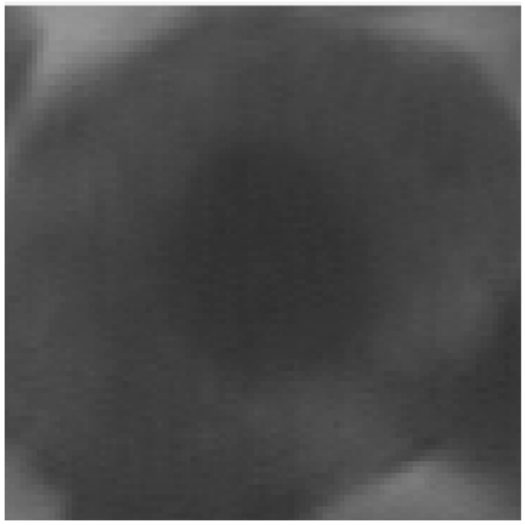

Fig. 6. Grayscale converted image.

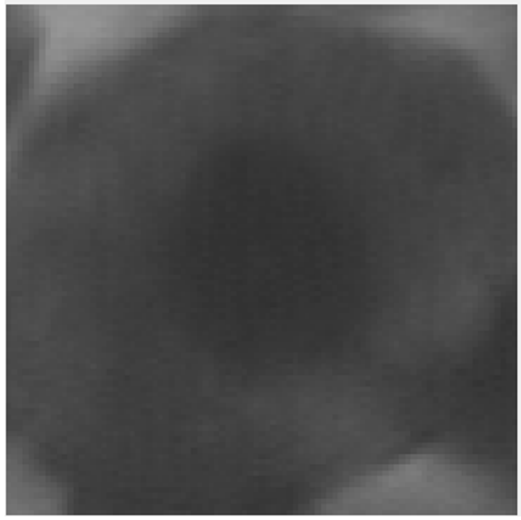

Fig. 7. Bilateral smoothened image.

Table IV presents the comparative accuracy values of various deep learning models used for cervical cell classification. The accuracy metric provides a general measure of correct predictions over the total predictions and is critical in medical diagnostics. It is observed that the proposed PapEMS-Net model outperforms all other methods. Figure 13 visualizes these accuracy scores through a hatched bar plot, where the proposed model is distinctly colored, making its superior performance visually apparent. This clear differentiation in both the table and the chart underscores the robustness and reliability of the PapEMS-Net architecture in high-precision classification tasks.

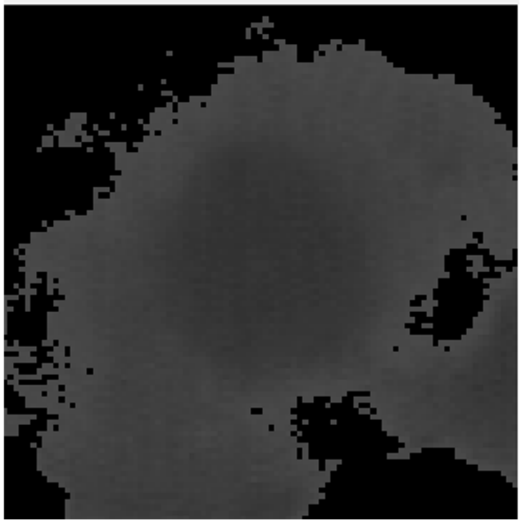

Fig. 8. Intensity-based thresholding.

Fig. 9. Sobel-based edge detection.

Fig. 10. Bridging using morphology.

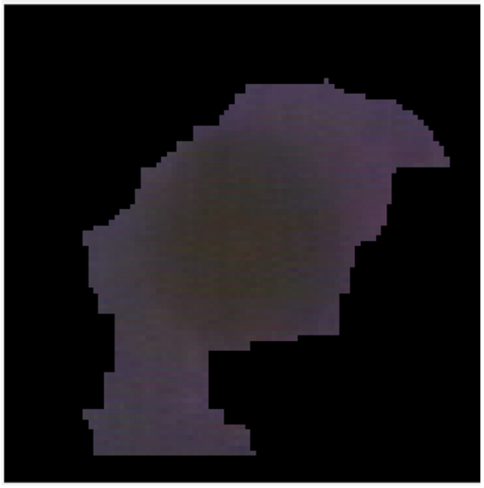

Fig. 11. Abnormality region of interest detected.

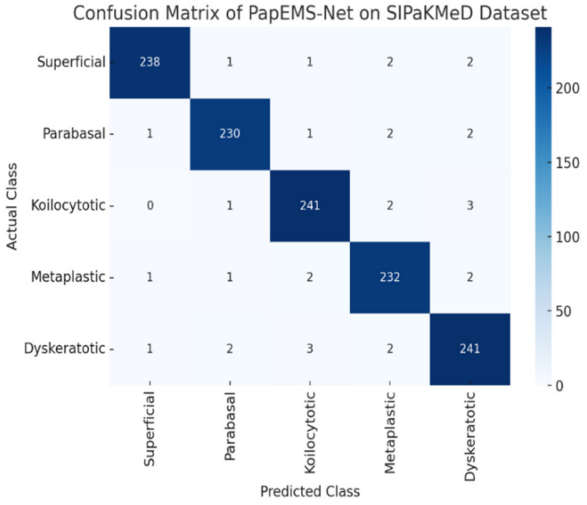

Fig. 12. Confusion matrix of the model.

TABLE IV. ACCURACY COMPARISON

Model name	Accuracy (%)
ResNet-50 + VGG-19 [23]	94.53
EfficientNet + Attention [24]	98.45
ResNet-152 [25]	98.08
CCanNet (CNN + ViT) [26]	98.53
SqueezeNet [27]	91.20
GCN [28]	99.11
DenseNet121 + Self-Attention [29]	95.00
MSENet [30]	97.21
Proposed PapEMS-Net	99.43

Table V details the precision values across different models, which reflect the ability of the classifier to correctly identify only the relevant class samples without mislabeling negatives. The proposed PapEMS-Net achieves the highest precision at 99.29%, followed by GCN at 99.09%, and CCanNet at 98.00%. Figure 14 provides a visual comparison of the precision values, with the proposed model again marked

prominently in orange. The plot reinforces the table's findings by emphasizing the lead maintained by PapEMS-Net in minimizing classification errors. Table VI compares the recall percentages of each model, indicating how well each method retrieves all relevant instances from the dataset. The proposed PapEMS-Net achieves a recall of 99.37%, which is the highest among all compared models, slightly ahead of GCN at 99.14%. Figure 15 illustrates these values in a bar chart where PapEMS-Net again shows a prominent lead, reinforcing its effectiveness in comprehensive cell detection.

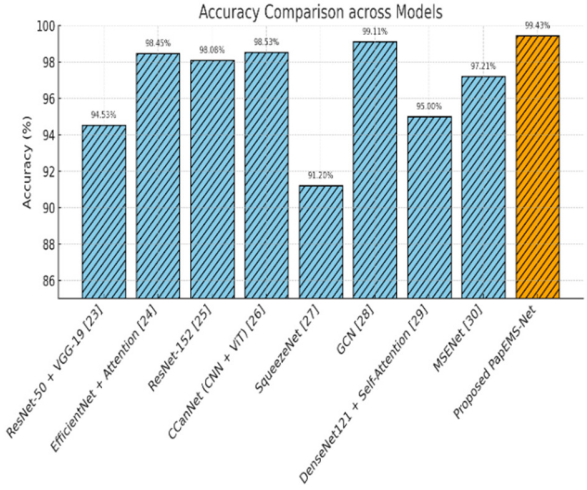

Fig. 13. Accuracy comparison plot.

TABLE V. PRECISION COMPARISON

Model name	Precision (%)
EfficientNet + Attention [24]	97.92
ResNet-152 [25]	91.62
CCanNet (CNN + ViT) [26]	98.00
GCN [28]	99.09
DenseNet121 + Self-Attention [29]	92.00
Proposed PapEMS-Net	99.29

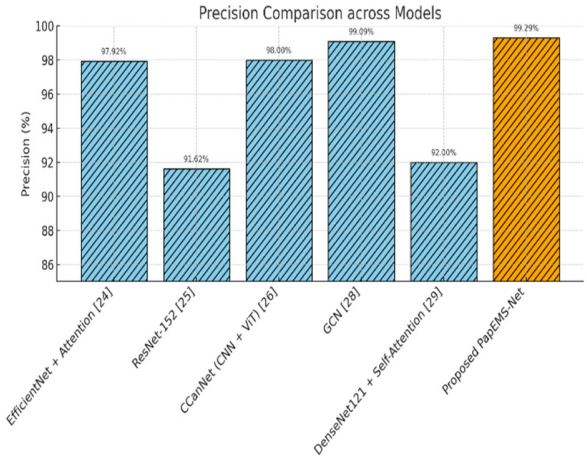

Fig. 14. Precision comparison plot.

TABLE VI. RECALL COMPARISON

Model name	Recall (%)
EfficientNet + Attention [24]	95.00
ResNet-152 [25]	91.61
GCN [28]	99.14
DenseNet121 + Self-Attention [29]	92.00
Proposed PapEMS-Net	99.37

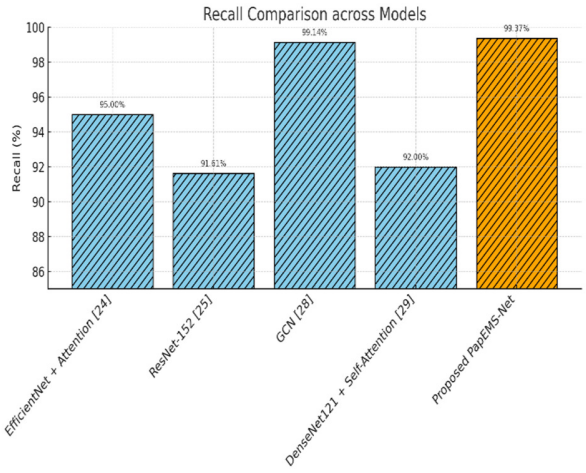

Fig. 15. Recall comparison plot.

Table VII highlights the F1 Score comparison, where PapEMS-Net achieves an F1 Score of 99.31%, outperforming all other models in the list. GCN and CCanNet also perform well with scores of 99.12% and 99.00%, respectively. Figure 16 illustrates the F1 scores, with the proposed model again standing out in orange, showcasing its superiority in achieving both high sensitivity and specificity in classification.

TABLE VII. F1 SCORE COMPARISON

Model name	F1 Score (%)
ResNet-50 + VGG-19 [23]	93.00
EfficientNet + Attention [24]	96.14
CCanNet (CNN + ViT) [26]	99.00
GCN [28]	99.12
DenseNet121 + Self-Attention [29]	92.00
Proposed PapEMS-Net	99.31

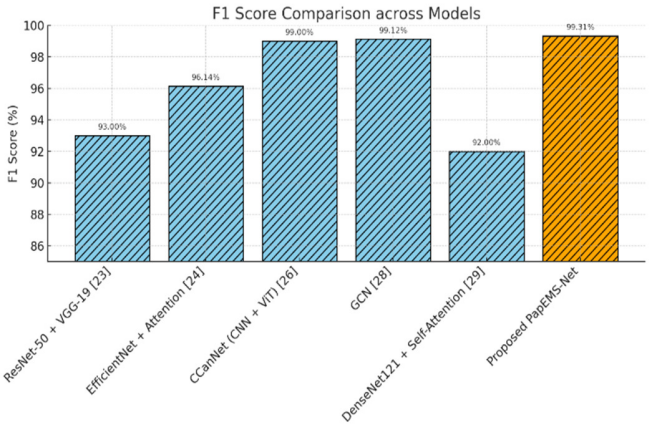

Fig. 16. F1 Score comparison plot.

Figure 17 displays the class-wise distribution of the detected cervical cell types, as predicted by the PapEMS-Net model, represented in a donut chart format. This plot reflects how the model has categorized the test samples across the five major cell classes. When this distribution is compared with Figure 3, which represents the ground truth class distribution in the SIPaKMeD dataset, the differences are subtle but important. Figure 3 demonstrates a near-even spread around 20% for each class, a result of careful dataset curation. In contrast, Figure 17 reveals slight classification deviations, especially an under-prediction of Koilocytotic cells and an over-representation of Metaplastic cells.

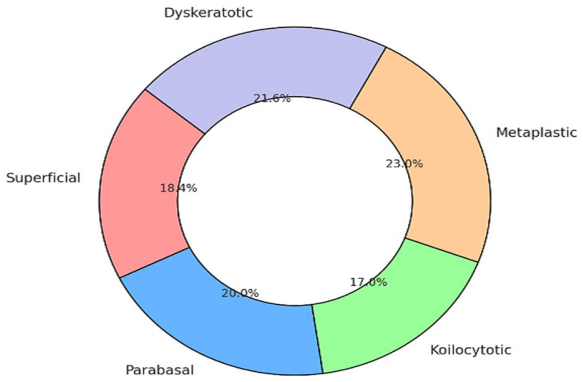

Fig. 17. Class distribution of detected cases by PapEMS-Net (Donut view).

During the model development, key challenges included handling inter-class similarity among cell types, managing overlapping cell structures in PAP smear images, and ensuring generalization across different sample variations. Additionally, balancing computational efficiency with high classification accuracy was critical for making the model practical for real-world use.

V. CONCLUSION

The experimental results and visual validations presented in this study confirm that the proposed PAP smear EfficientNet-MVO-Softmax classifier Network (PapEMS-Net) model offers a highly accurate, efficient, and interpretable solution for the automated classification of cervical cells in PAP smear images. By combining the feature extraction capabilities of EfficientNet, the optimization potential of the Multi-Verse Optimizer (MVO), and a robust Softmax Entropy Classifier, the model achieved outstanding results with an accuracy of 99.43%, precision of 99.29%, recall of 99.37%, and F1-score of 99.31%. It maintained strong class-wise performance with ROC AUC values close to 95% across all five categories and predicted cell distributions with only minor deviations (±3%) from the actual class proportions. In future work, PapEMS-Net can be extended by incorporating explainable AI techniques to improve interpretability and by integrating additional imaging modalities for broader applicability. Furthermore, its deployment on lightweight edge devices would enable real-time use in low-resource clinical settings, making the system practical for widespread adoption.

DATASET AVAILABILITY

The dataset used in this study is publicly available at: https://www.kaggle.com/datasets/prahladmehandiratta/cervical-cancer-largest-dataset-sipakmed.

REFERENCES

[1] Z. Alyafeai and L. Ghouti, "A Fully-automated Deep Learning Pipeline for Cervical Cancer Classification," *Expert Systems with Applications*, vol. 141, Mar. 2020, Art. no. 112951, https://doi.org/10.1016/j.eswa.2019.112951.

[2] L. Zhe Wei, W. Azani Mustafa, M. Aminudin Jamlos, S. Zulkarnain Syed Idrus, and M. Hamzari Sahabudin, "Cervical Cancer Classification Using Image Processing Approach: A Review," *IOP Conference Series: Materials Science and Engineering*, vol. 917, no. 1, Sept. 2020, Art. no. 012068, https://doi.org/10.1088/1757-899X/917/1/012068.

[3] R. L. Siegel, K. D. Miller, N. S. Wagle, and A. Jemal, "Cancer Statistics, 2023," *CA: A Cancer Journal for Clinicians*, vol. 73, no. 1, pp. 17–48, Jan. 2023, https://doi.org/10.3322/caac.21763.

[4] M. S. Balkin, "Cervical Cancer Prevention and Treatment: Science, Public Health and Policy Overview," in *Challenges and Opportunities for Women's Right to Health*, Brussels, Belgium, Sept. 2007.

[5] T. Šarenac and M. Mikov, "Cervical Cancer, Different Treatments and Importance of Bile Acids as Therapeutic Agents in This Disease," *Frontiers in Pharmacology*, vol. 10, June 2019, Art. no. 484, https://doi.org/10.3389/fphar.2019.00484.

[6] H. Basak, R. Kundu, S. Chakraborty, and N. Das, "Cervical Cytology Classification Using PCA and GWO Enhanced Deep Features Selection," *SN Computer Science*, vol. 2, no. 5, Sept. 2021, Art. no. 369, https://doi.org/10.1007/s42979-021-00741-2.

[7] P. Oak, P. S. Deshpande, and B. Iyer, "A Deep Learning-Driven Multimodal Healthcare System for the Early Detection of Cervical Cancer," *Engineering, Technology & Applied Science Research*, vol. 15, no. 4, pp. 24328–24333, Aug. 2025, https://doi.org/10.48084/etasr.11277.

[8] S. L. Bedell, L. S. Goldstein, A. R. Goldstein, and A. T. Goldstein, "Cervical Cancer Screening: Past, Present, and Future," *Sexual Medicine Reviews*, vol. 8, no. 1, pp. 28–37, Jan. 2020, https://doi.org/10.1016/j.sxmr.2019.09.005.

[9] N. Dong, L. Zhao, C. H. Wu, and J. F. Chang, "Inception v3 Based Cervical Cell Classification Combined with Artificially Extracted Features," *Applied Soft Computing*, vol. 93, Aug. 2020, Art. no. 106311, https://doi.org/10.1016/j.asoc.2020.106311.

[10] U. E. Akpudo and J.-W. Hur, "D-dCNN: A Novel Hybrid Deep Learning-Based Tool for Vibration-Based Diagnostics," *Energies*, vol. 14, no. 17, Aug. 2021, Art. no. 5286, https://doi.org/10.3390/en14175286.

[11] K. P. Win, Y. Kitjaidure, K. Hamamoto, and T. Myo Aung, "Computer-Assisted Screening for Cervical Cancer Using Digital Image Processing of Pap Smear Images," *Applied Sciences*, vol. 10, no. 5, Mar. 2020, Art. no. 1800, https://doi.org/10.3390/app10051800.

[12] T. Zhang *et al.*, "Cervical Precancerous Lesions Classification Using Pre-Trained Densely Connected Convolutional Networks with Colposcopy Images," *Biomedical Signal Processing and Control*, vol. 55, Jan. 2020, Art. no. 101566, https://doi.org/10.1016/j.bspc.2019.101566.

[13] W. Hua *et al.*, "Lymph-vascular Space Invasion Prediction in Cervical Cancer: Exploring Radiomics and Deep Learning Multilevel Features of Tumor and Peritumor Tissue on Multiparametric MRI," *Biomedical Signal Processing and Control*, vol. 58, Apr. 2020, Art. no. 101869, https://doi.org/10.1016/j.bspc.2020.101869.

[14] A. Khamparia, D. Gupta, J. J. P. C. Rodrigues, and V. H. C. De Albuquerque, "DCAVN: Cervical Cancer Prediction and Classification Using Deep Convolutional and Variational Autoencoder Network," *Multimedia Tools and Applications*, vol. 80, no. 20, pp. 30399–30415, Aug. 2021, https://doi.org/10.1007/s11042-020-09607-w.

[15] T. I. Yusufaly *et al.*, "A Knowledge-based Organ Dose Prediction Tool for Brachytherapy Treatment Planning of Patients with Cervical

Cancer," *Brachytherapy*, vol. 19, no. 5, pp. 624–634, Sept. 2020, https://doi.org/10.1016/j.brachy.2020.04.008.

[16] S. I. Kim, S. Lee, C. H. Choi, M. Lee, J. W. Kim, and Y. B. Kim, "Prediction of Disease Recurrence According to Surgical Approach of Primary Radical Hysterectomy in Patients with Early-stage Cervical Cancer Using Machine Learning Methods," *Gynecologic Oncology*, vol. 159, pp. 185–186, Oct. 2020, https://doi.org/10.1016/j.ygyno.2020.05.283.

[17] M. Suriya, V. Chandran, and M. G. Sumithra, "Enhanced Deep Convolutional Neural Network for Malarial Parasite Classification," *International Journal of Computers and Applications*, vol. 44, no. 12, pp. 1113–1122, Dec. 2022, https://doi.org/10.1080/1206212X.2019.1672277.

[18] T. A. Kessler, "Cervical Cancer: Prevention and Early Detection," *Seminars in Oncology Nursing*, vol. 33, no. 2, pp. 172–183, May 2017, https://doi.org/10.1016/j.soncn.2017.02.005.

[19] Y. R. Park, Y. J. Kim, W. Ju, K. Nam, S. Kim, and K. G. Kim, "Comparison of Machine and Deep Learning for the Classification of Cervical Cancer Based on Cervicography Images," *Scientific Reports*, vol. 11, no. 1, Aug. 2021, Art. no. 16143, https://doi.org/10.1038/s41598-021-95748-3.

[20] E. Hussain, L. B. Mahanta, C. R. Das, and R. K. Talukdar, "Comparison of Machine and Deep Learning for the Classification of Cervical Cancer Based on Cervicography Images," *Tissue and Cell*, vol. 65, Aug. 2020, Art. no. 101347, https://doi.org/10.1016/j.tice.2020.101347.

[21] M. E. Plissiti, M. Vrigkas, and C. Nikou, "Segmentation of Cell Clusters in Pap Smear Images Using Intensity Variation Between Superpixels," in *2015 International Conference on Systems, Signals and Image Processing*, London, United Kingdom, Sept. 2015, pp. 184–187, https://doi.org/10.1109/IWSSIP.2015.7314207.

[22] N. Zamanitajeddin, M. Jahanifar, M. Bilal, M. Eastwood, and N. Rajpoot, "Social Network Analysis of Cell Networks Improves Deep Learning for Prediction of Molecular Pathways and Key Mutations in Colorectal Cancer," *Medical Image Analysis*, vol. 93, Apr. 2024, Art. no. 103071, https://doi.org/10.1016/j.media.2023.103071.

[23] A. K. Sharma, A. Nandal, A. Dhaka, A. Alhudhaif, K. Polat, and A. Sharma, "Diagnosis of Cervical Cancer Using CNN Deep Learning Model with Transfer Learning Approaches," *Biomedical Signal Processing and Control*, vol. 105, July 2025, Art. no. 107639, https://doi.org/10.1016/j.bspc.2025.107639.

[24] Y. Dogan, "AutoEffFusionNet: A New Approach for Cervical Cancer Diagnosis Using ResNet-Based Autoencoder with Attention Mechanism and Genetic Feature Selection," *IEEE Access*, vol. 13, pp. 44107–44122, 2025, https://doi.org/10.1109/ACCESS.2025.3543850.

[25] S. K. Mathivanan, D. Francis, S. Srinivasan, V. Khatavkar, K. P, and M. A. Shah, "Enhancing Cervical Cancer Detection and Robust Classification Through a Fusion of Deep Learning Models," *Scientific Reports*, vol. 14, no. 1, May 2024, Art. no. 10812, https://doi.org/10.1038/s41598-024-61063-w.

[26] Md. H. K. Mehedi, M. Khandaker, S. Ara, Md. A. Alam, M. F. Mridha, and Z. Aung, "A Lightweight Deep Learning Method to Identify Different Types of Cervical Cancer," *Scientific Reports*, vol. 14, no. 1, Nov. 2024, Art. no. 29446, https://doi.org/10.1038/s41598-024-79840-y.

[27] M. H. Sadananda, "Cervical Cancer Detection with a Tissue Smear and a Microscopic Image inside the Deep Learning Model of Squeeze Net," *International Journal for Research in Applied Science and Engineering Technology*, vol. 12, no. 5, pp. 4434–4437, May 2024, https://doi.org/10.22214/ijraset.2024.62579.

[28] N. M. Fahad, S. Azam, S. Montaha, and Md. S. H. Mukta, "Enhancing Cervical Cancer Diagnosis with Graph Convolution Network: Ai-powered Segmentation, Feature Analysis, and Classification for Early Detection," *Multimedia Tools and Applications*, vol. 83, no. 30, pp. 75343–75367, Feb. 2024, https://doi.org/10.1007/s11042-024-18608-y.

[29] B. Z. Wubineh, A. Rusiecki, and K. Halawa, "Classification of Cervical Cells from the Pap Smear Image Using the RES_DCGAN Data Augmentation and ResNet50V2 with Self-attention Architecture," *Neural Computing and Applications*, vol. 36, no. 34, pp. 21801–21815, Dec. 2024, https://doi.org/10.1007/s00521-024-10404-x.

[30] R. Pramanik, B. Banerjee, and R. Sarkar, "MSENet: Mean and Standard Deviation Based Ensemble Network for Cervical Cancer Detection," *Engineering Applications of Artificial Intelligence*, vol. 123, Aug. 2023, Art. no. 106336, https://doi.org/10.1016/j.engappai.2023.106336.

[31] M. E. Plissiti, P. Dimitrakopoulos, G. Sfikas, C. Nikou, O. Krikoni, and A. Charchanti, "Sipakmed: A New Dataset for Feature and Image Based Classification of Normal and Pathological Cervical Cells in Pap Smear Images," in *2018 25th IEEE International Conference on Image Processing*, Athens, Oct. 2018, pp. 3144–3148, https://doi.org/10.1109/ICIP.2018.8451588.

AUTHORS PROFILE

Ms. M. Sandhya Vani received her M.Tech degree from NRI Institute of Technology, Hyderabad, in 2014 and her B.Tech degree from P. R. R. M Engineering College, Hyderabad, in 2009. She is currently a Research Scholar, pursuing her Ph.D. in the Department of Computer Science and Engineering, Koneru Lakshmaiah Education Foundation, Hyderabad-500075, Telangana, India.

Rama Rao N is a distinguished professional in Computer Science and Engineering, holding a Ph.D. from JNTUH, with over 25 years of experience in software development, teaching, and research. He worked in product development for more than three years, honing his skills in Shell scripting, C, Java, J2EE, and using frameworks, such as Struts and SAP Portal implementation. His extensive track record includes more than 20 years of providing comprehensive training and knowledge transfer to various individuals, along with two years of sales and service experience, demonstrating adaptability. His expertise spans full-stack development using Python, Machine Learning, and networking and cloud security.